IOP Publishing Measurement Science and Technology
Meas. Sci. Technol. **31** (2020) 065010 (7pp) https://doi.org/10.1088/1361-6501/ab75b0

Extending voltage range to 10 V rms in AC–DC difference measurements with AC programmable Josephson voltage standard

Yasutaka Amagai[1], Michitaka Maruyama[1], Hirotake Yamamori[2], Takeshi Shimazaki[1], Kenjiro Okawa[1], Hiroyuki Fujiki[1] and Nobu-Hisa Kaneko[1]

[1] National Metrology Institute of Japan (NMIJ), National Institute of Advanced Industrial Science and Technology (AIST), Tsukuba 305-8563, Japan
[2] Nanoelectronics Research Institute (NeRI), National Institute of Advanced Industrial Science and Technology (AIST), Tsukuba 305-8568, Japan

E-mail: y-amagai@aist.go.jp

Received 9 August 2019, revised 8 January 2020
Accepted for publication 12 February 2020
Published 31 March 2020

Abstract

The larger-scale programmable Josephson voltage standard (PJVS) chip composed of 524 288 niobium nitride-based overdamped Josephson junctions enables us to generate stepwise-approximated AC waveforms with a root-mean-square (rms) amplitude of up to 10 V. In this study, we have extended the voltage range of the differential sampling system based on the AC-PJVS to an rms value of 10 V with the larger-scale PJVS chip. The sampling digital voltmeter (DVM) that is employed to measure differential voltages is modified to use a 10 MHz reference clock instead of an internal clock. This modification substantially improves the uncertainty of AC–DC difference measurements at low frequencies, which is caused by the internal clock error of the sampling DVM, by preventing the incoherent sampling of the differential voltages. The expanded uncertainties ($k = 2$) of the AC–DC difference measurements are reduced from 7.0 μV/V to 1.8 μV/V for a frequency of 62.5 Hz and from 8.0 μV/V to 4.4 μV/V for a frequency of 1 Hz. The improvements in the uncertainty are more significant compared with a conventional method at low frequencies, where the accuracy of a thermal voltage converter is reduced.

Keywords: AC voltage metrology, AC–DC difference measurement, thermal voltage converter, Josephson effect

(Some figures may appear in colour only in the online journal)

1. Introduction

AC voltage is calibrated by comparing the Joule heat of an unknown AC voltage with that of a known DC voltage using a thermal voltage converter (TVC) in a frequency range of 10 Hz to 100 MHz [1]. The AC–DC difference, which is defined as the difference in the response of the TVC to AC and DC signals, is indispensable for accurately determining the root-mean-square (rms) value of an AC sinusoidal waveform. However, it is difficult to theoretically accurately evaluate the low-frequency AC–DC difference below 10 Hz because of the complex heat transfer of the TVC caused by Joule heating oscillations, the change in the electrical resistance of a heater, and the nonlinear heat transfer of the TVC [2–4]. Direct sampling methods are widely used for calibrating AC voltage in a frequency range below 10 Hz [5–8]. However, the accuracy of these methods is limited by the undesirable gain errors and nonlinearity effects of sampling voltmeters. AC programmable Josephson voltage standards (AC-PJVS) with rapid settling times [9] and intrinsically stable

voltage steps have been developed to satisfy the requirements for improved low-frequency AC metrology [10, 11]. A calculable rms stepwise-approximated sinusoidal waveform is generated using binary-segmented Josephson arrays in such a manner that the voltage at each step has quantum accuracy. Such a calculable stepwise-approximated waveform generated by the AC-PJVS is promising for the experimental evaluation of the low-frequency AC–DC difference of a TVC. However, in this technique, the nonzero rise times of electronic bias circuits influence step transitions [12–14]. In addition, the load current provided by the AC-PJVS is not sufficient to drive a conventional TVC with a nominal current of approximately 5 mA or 10 mA. To address these technical issues, a variety of measurement techniques have been developed to evaluate the AC–DC difference of a TVC [15–19]. These techniques are divided into two broad categories: differential sampling techniques, which use a semiconductor AC/DC source [20, 21], and techniques involving the direct application of stepwise-approximated waveforms via a precision amplifier [22, 23]. Differential sampling techniques are particularly useful because they eliminate the errors caused by the finite transitions between quantized voltage steps. The semiconductor AC/DC source in a differential configuration is capable of supplying signal and load currents to a TVC.

Previously, a differential sampling measurement system capable of producing an rms amplitude of 3 V and performing TVC measurements was developed using the AC-PJVS for low-frequency applications down to 1 Hz [24]. The goal of our study is to eventually replace the conventional system by the differential sampling system based on the AC-PJVS for reduced uncertainties. However, the requirements for the calibration of AC voltmeters, calibrators, and TVCs down to 1 Hz up to an rms amplitude of 10 V continue to increase owing to the widespread dissemination of mechanical vibration and infrasonic sensor calibrations.

This work aims to extend the voltage range of the differential sampling system based on the AC-PJVS to an rms value of 10 V at a frequency down to 1 Hz. Additionally, this study aims to reduce the undesirable effects that arise from the internal clock error of a sampling digital voltmeter (DVM) using a 10 MHz reference clock to synchronize the AC-PJVS system and semiconductor AC/DC source.

2. Measurement setup and principle

The main components of the measurement setup were the AC-PJVS system, the semiconductor AC/DC source (Fluke 5720A and 5520A) that supplied current to TVCs, and the sampling DVM (Keysight 3458A).

2.1. AC-programmable Josephson voltage standard

The PJVS chip is composed of 524 288 niobium nitride-based overdamped Josephson junction arrays operated with a Gifford–McMahon cooler at 10 K [25]. The temperature fluctuation of the cold head due to the cooler operation was approximately within ± 50 mK in a 1 Hz cycle. The bias

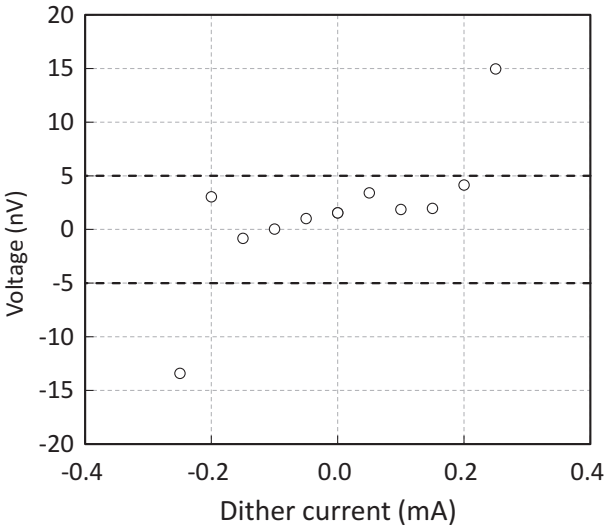

Figure 1. Typical measurement result of the flatness of a quantized voltage step with DC dither currents simultaneously applied for all junctions used for a 10 V rms AC waveform in a back-to-back configuration. Each point indicates the averaged value of the normal and reverse polarities of the bias currents. Dotted line indicates a threshold value of 5 nV, which may correspond to the maximum height of the measurement noise in our setup.

operating points in our PJVS system may be affected by the self-heating effect of the chip with a large number of junctions. Therefore, we conducted a heat transfer analysis of the proposed chip module and obtained the optimized operating conditions [26]. Figure 1 depicts the typical measurement result of a quantized voltage step with dither currents simultaneously applied for all junctions used for generating an AC waveform. The junction array consisted of two sets of 12 binary segments, each of which was laid out symmetrically. This enabled us to carry out back-to-back measurements. The current source simultaneously biased the half-array at the negative Shapiro step (–7 V) and the other half-array at the positive Shapiro step (7 V), which canceled the output voltage. Thus, the nanovoltmeter (Keysight 34420A) only measured the thermoelectric voltage on the quantized step, suppressing the effect of the gain error. A polarity reversal of the bias current was applied to this measurement for eliminating the offset error due to the thermoelectric voltage. A DC dither current was applied to the full array to measure the quantized-step width, i.e. the operating margin. Herein, the dither current is defined as the difference between the bias current applied to each junction and the bias current optimized for the center of each voltage step. From figure 1, it was confirmed that the fabricated chip had an operating margin of ± 0.2 mA.

2.2. Differential sampling measurement

Figure 2 depicts a schematic of the sampling measurement setup. In our measurement setup, the AC-PJVS system calibrated a semiconductor AC/DC source that supplied signal and load currents to the TVC. The Fluke 5720A commercial calibrator was used as the AC source for a frequency range above 10 Hz and the DC source, and Fluke 5520A was used

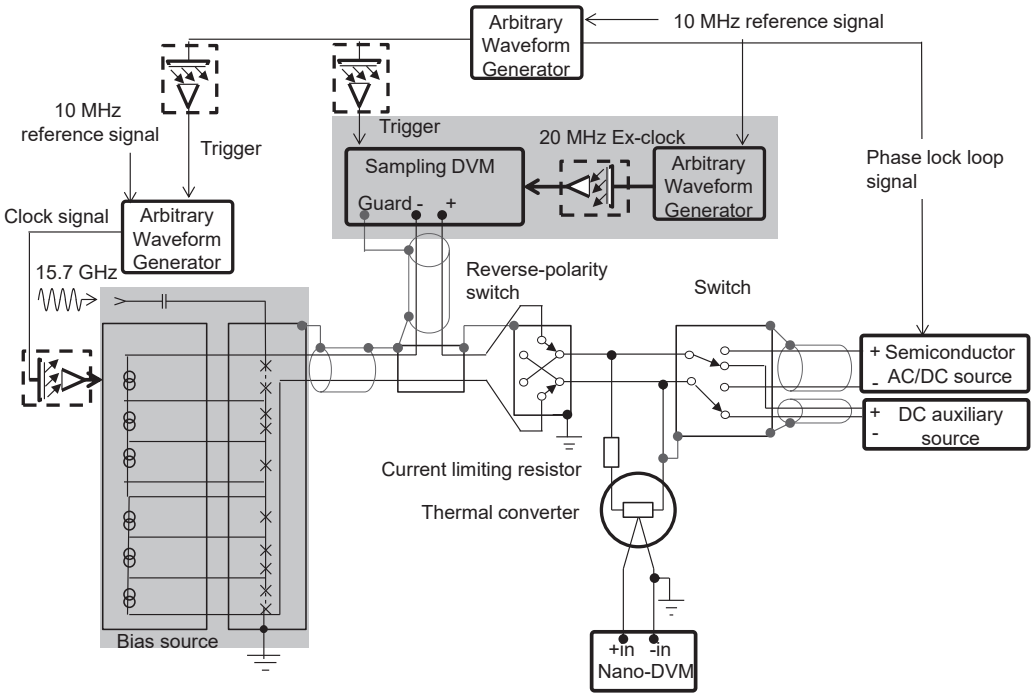

Figure 2. Schematic of the measurement setup for evaluating the TVC based on the AC-PJVS system (highlighted in grey) using the larger-scale PJVS chip that allows for outputs at an rms value of 10 V. The sampling digital voltmeter (DVM) highlighted in grey was modified to be locked with an external 20 MHz clock signal via an optical isolator, unlike our previous setup for the AC–DC difference measurement at 3 V © 2013 IEEE. Reprinted, with permission, from [24].

as the AC source for a frequency range below 10 Hz and the DC source. There were eight steps per cycle in the AC-PJVS stepwise-approximated waveforms. The signals generated by the AC-PJVS system for reconstructing the sinusoidal waveform were the on-step samples. Hence, the delay time of the sampling DVM was optimized to minimize the differential voltage in a fixed aperture time. The typical values for the aperture time were 1 ms, 6.25 ms, and 62.5 ms for frequencies of 62.5 Hz, 10 Hz, and 1 Hz, respectively. The optimized delay times were 14.983 ms, 91 ms, and 910 ms. These differential sampling procedures were the same as those used in our previous measurement for 3 V rms [24]. With eight samples per period at an rms amplitude of 10 V, the input stages of the sampling DVM were overloaded most of the time if the 1-V range or 100-mV range of the sampling DVM was selected. Recovery from overload is gradual, and it affects the results. Thus, the 10-V range of the sampling DVM was selected. The specified gain correction error of the 10-V range of the sampling DVM was acceptable for the AC–DC measurements. In the previous differential sampling system, the stepwise approximated AC waveform generated from the AC-PJVS system was synchronized with the AC source using a master-clock synthesizer to prevent the misalignment of the two waveforms. However, the sampling DVM used as a null detector was referred to its internal clock to measure the differential voltages. Therefore, we modified the sampling DVM so that it could be locked to an external clock to prevent the incoherent sampling of the differential voltages. All generated clock input clock signals were locked to the same 10 MHz reference. Moreover, all signals for synchronization, which were generated from arbitrary waveform generators, were optically isolated from the three main components to reduce the noise level and prevent redundant ground connections. A reverse-polarity relay switch was used to invert the sinusoidal waveform to be sampled for canceling out the thermal offset voltage in the signal cables. This enabled us to reconstruct a full waveform with information related to a possible asymmetrical distortion of the measured waveform.

2.3. AC–DC difference measurement

When the AC and DC voltage inputs to the TVC were approximately the same, the AC–DC voltage transfer difference, δ, could be calculated as follows [24]:

$$\delta_{\mathrm{AC-DC}} = \frac{V_{\mathrm{AC}} - V_{\mathrm{DC}}}{V_{\mathrm{DC}}} - \frac{E'_{\mathrm{AC}} - E'_{\mathrm{DC}}}{nE'_{\mathrm{DC}}}, \tag{1}$$

$$n \equiv \frac{\mathrm{d}E}{E} \Big/ \frac{\mathrm{d}V}{V} = \frac{\mathrm{d}E}{\mathrm{d}V}\frac{V_{\mathrm{DC}}}{E_{\mathrm{DC}}}, \tag{2}$$

$$E'_{\mathrm{DC}} = \frac{E'_{DC+} + E'_{\mathrm{DC}-}}{2}. \tag{3}$$

Here, E_{DC} and E_{AC} represent the output voltages of the thermocouple in the TVC when the rms DC and AC voltages, V_{DC} and V_{AC}, respectively, are applied. n is a normalized index that indicates the square characteristics of the input–output responses of a thermal converter, and it is approximately 2

in numerous cases. Note that E'_{DC} is the mean value when a DC voltage with positive and negative polarities is applied, as in (3).

The TVC, which used planar multijunction thermal converters (PMJTCs), was fabricated. The heater resistance of the PMJTC was 80 Ω, with a nominal current of 10 mA. To evaluate these devices at an rms voltage of 10 V, current-limiting resistors of 1 kΩ were connected in series with the PMJTC. The measurement sequence of the AC–DC difference in the TVC was AC, DC-positive, DC-negative, and AC The delay in the TVC measurements between the AC and DC operations was 10 s. The total measurement time, including the waiting time, for one AC–DC difference measurement was approximately 270 s. Before beginning the measurement sequence, a waiting time of approximately 20 min was required to reduce the thermal drift to 0.1 ppm min^{-1}. The output voltage data from the thermocouple were integrated after a waiting time of 10 s. The measurement process was repeated ten times. The applied voltage was 10 V, and the measurements were performed at frequencies ranging from 1 Hz to 100 Hz.

In the above-mentioned sequence, the output voltage from the thermocouple in the TVC was measured using a nanovoltmeter (Keysight 34420A). If the amplitude of the input voltage is constant and its period is shorter than the thermal time constant of the TVC, the heater temperature is constant. As the period of the input voltage increases and approaches the thermal time constant of the TVC, the heater temperature begins to track the square of the instantaneous input voltage. Thus, the temperature variation in the heater in the TVC becomes negligible at low frequencies [1, 2]. Even in such situations, the precise DC components of the output voltage from the thermocouple were obtained by selecting the integration period of the nanovoltmeter to cover an integer number of signal periods of the thermocouple in the TVC.

3. Experimental results

3.1. AC–DC difference of a TVC

One of the advantages of the differential sampling measurement method is its ability to calibrate the TVCs even in a frequency range below 10 Hz. In this study, we focused on the evaluation of the frequency dependence of the AC–DC difference of the TVC in a frequency range down to 1 Hz. Figure 3 shows the obtained AC–DC differences in a frequency range of 1 Hz to 62.5 Hz. The measured AC–DC differences increased as the frequency decreased and approached 1 Hz. This behavior is consistent with the thermal time constant of the PMJTC of approximately 1 s, which was estimated in our preliminary measurement. As seen in the inset of figure 3, the standard deviation of the mean of the measured AC–DC differences increased as the frequency decreased below 10 Hz. The values of the standard deviation of the mean were approximately 1.1 μV/V at 10 Hz and 2.3 μV/V at 1 Hz. Even though all measurements were carefully timed in the differential configuration, the temperature vibrations in the heater of the TVC, the semiconductor AC/DC source jitter, and the noise and output stability of the TVC are inherent contributors to type-A uncertainty in the AC–DC difference measurement. In particular, the large increase in the standard deviation of the AC–DC difference most likely reflects the temperature variations in the heater in the PMJTC. This is because of the finite thermal mass, as the standard deviation of the input voltage to the TVC from a semiconductor AC/DC source still remains within a few parts in 10^{-6} in the measured frequency range down to 1 Hz.

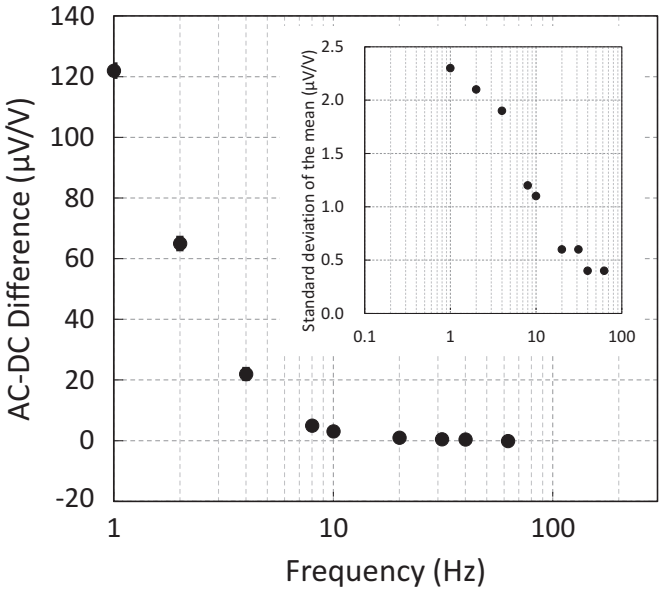

Figure 3. Frequency dependence of the AC–DC difference in a frequency range of 1 Hz to 62.5 Hz at an rms voltage of 10 V. The inset shows the standard deviation of the mean ($k = 1$).

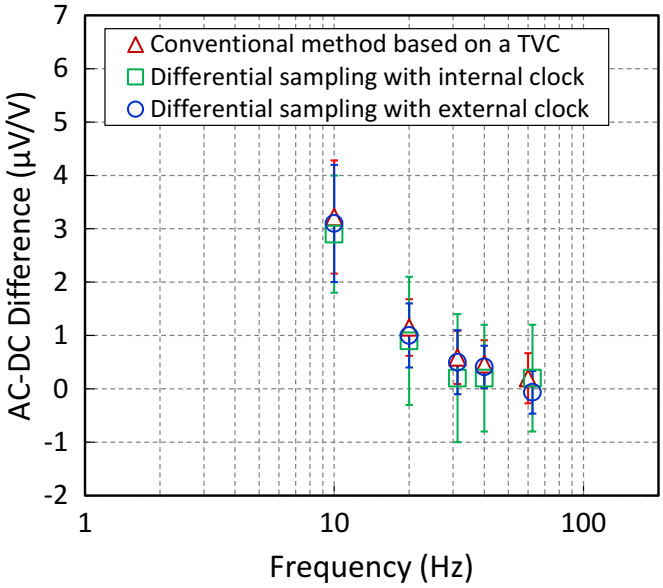

Figure 4. Comparison of the AC–DC differences obtained by three different setups; a conventional AC–DC comparison method, the differential sampling along with the sampling DVM referred to its internal clock, and the differential sampling method along with sampling DVM referred to the external clock (present study) at an rms value of 10 V. The error bars represent the standard deviation of the mean ($k = 1$) obtained from ten repeated measurements.

Table 1. Expanded uncertainty of AC–DC differences at rms value of 10 V and frequency of 62.5 Hz obtained by three different setups.

Source of uncertainty	Type	Expanded uncertainty (μV/V)		
		Thermal converter	Differential sampling along with sampling DVM referred to its internal clock	Differential sampling along with sampling DVM referred to the external clock (present study)
Standard deviation of the mean	A	0.4	1.0	0.5
Digital voltmeter (DVM) gain correction error	B	—	0.0	0.0
Effective common mode rejection ratio (CMRR)	B	—	0.1	0.1
Phase error	B	—	0.2	0.2
Thermal electromotive force	B	—	0.0	0.0
Timer error of sampling DVM	B	—	3.2	0.0
Reference thermal converter (voltage coefficient)	B	3.5	—	—
Voltage dependence	B	2.9	—	—
Temperature coefficient of the TVC	B	0.6	0.6	0.6
Stability of the AC source	B	0.4	0.4	0.4
Index n measurement	B	0.1	0.1	0.1
Resolution of nanovoltmeter	B	0.1	0.1	0.1
Combined standard uncertainty		4.7	3.5	0.9
Expanded uncertainty ($k = 2$)		9.4	7.0	1.8

3.2. Thermal converter verification

In order to validate the measurement results obtained by the differential sampling method based on the AC-PJVS, the AC–DC difference was compared with the value determined by the conventional method based on the TVC in a frequency range of 10 Hz to 62.5 Hz. The AC–DC difference of the PMJTC was calibrated using the primary standard of the National Metrology Institute of Japan (NMIJ). This knowledge of the calibrated value of the AC–DC difference was also used to precisely adjust the AC and DC voltage generated from the AC/DC semiconductor source in the AC–DC difference measurements. We measured the higher harmonics of the AC source used in the experiment to evaluate its spectral purity. The contributions from the second and third harmonics were −90.2 dBc and −97.8 dBc, respectively. Thus, the harmonic contributions were particularly small, and their contribution to the AC–DC difference measurement may be well below 0.01 μV/V. As shown in figure 4, an extremely good agreement was observed between the AC–DC differences obtained by the two different methods. The values differed by 0.2 μV/V in a frequency range of 10 Hz to 62.5 Hz, which was within the standard deviation of the mean (0.45 μV/V) obtained from ten repeated measurements. Next, these results were compared with those obtained by the differential sampling along with the sampling DVM referred to its internal clock. Notice that the AC–DC differences obtained by the three different methods agreed well within the standard deviation of the mean, even though there was a slight systematic difference. The data obtained by the differential sampling tended to be lower than those obtained using the conventional method based on the TVC. We leave this investigation for future work because the agreement with the data obtained by the conventional method is well within the expanded uncertainty ($k = 2$), as mentioned hereinafter. Nevertheless, an understanding of these data is important for further reducing the uncertainty.

3.3. Uncertainty of AC–DC difference measurement

Table 1 lists the major uncertainty components of the AC–DC difference measurement for an rms value of 10 V and a frequency of 62.5 Hz for the three different setups. The uncertainty of the AC–DC difference measurement obtained by the differential sampling along with the sampling DVM referred to its internal clock was estimated as follows: The uncertainty contributions critically depended on the timer error of the sampling DVM because the time-base error was directly converted into errors in voltage. The upper bound on the time-base error caused by the incoherent sampling of the differential voltages was calculated to be 5.5 μV/V, leading to a standard uncertainty of 3.2 μV/V assuming a rectangular distribution. The output voltage stability of the semiconductor AC/DC source can also be a component of uncertainty in the AC–DC difference measurement. The stability of the output voltage of the AC source during the AC–DC measurement was 0.36 μV/V. This value was considered to be the short-term drift of the calibrator during the AC–DC measurement. The typical temperature coefficient of the output voltage from the thermocouple of the TVC was 100 ppm K^{-1}, and the temperature stability of our air bath was less than 0.01 K. This provided a related uncertainty of 0.58 μV/V assuming a rectangular distribution. As a result, the expanded uncertainty was 7.0 μV/V ($k = 2$). In contrast, the aforementioned internal clock error of the sampling DVM was significantly improved by being locked to an external clock referred to a 10 MHz reference clock to be equal with the time base of the AC-PJVS. However, the evaluation of the phase error, i.e. the misalignment of the two waveforms, which is the largest contribution to the expanded uncertainty, was quite difficult. We estimated the phase error by considering the maximum deviation of the phase relationship between the semiconductor source and AC-PJVS. The maximum deviation was ± 0.4 μV/V [27], providing a standard uncertainty of 0.23 μV/V in the AC–DC difference

Table 2. Expanded uncertainty of AC–DC difference measurements at rms value of 10 V for different frequencies.

Method	Expanded uncertainty in μV/V ($k = 2$)		
	1 Hz	10 Hz	62.5 Hz
Conventional method based on a TVC	—	30	9.4
Differential sampling along with a DVM referred to its internal clock	8.0	7.0	7.0
Differential sampling along with a DVM referred to the external clock (present study)	4.4	2.6	1.8

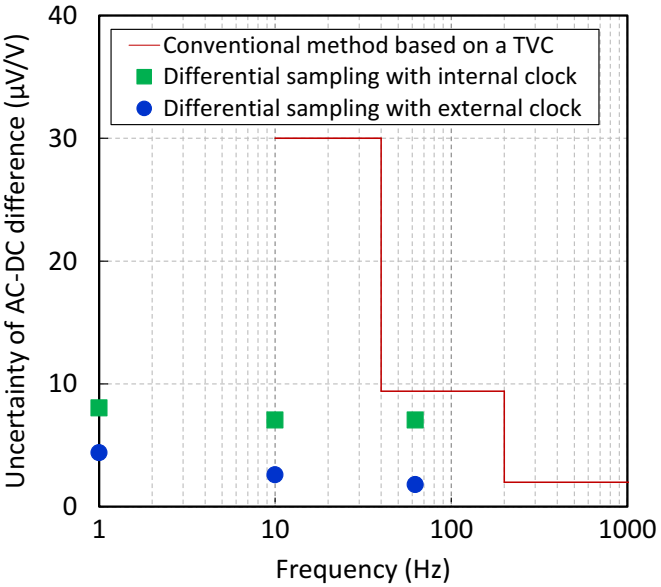

Figure 5. Expanded uncertainty of AC–DC difference measurement ($k = 2$) obtained by the three different setups at an rms value of 10 V.

measurements. As a result, the overall expanded uncertainty was evaluated to be 1.8 μV/V ($k = 2$). Next, we compared our result with those obtained by the conventional method based on the TVC. The routine NMIJ uncertainty of the AC–DC difference measurement was 9.4 μV/V ($k = 2$) for an rms value of 10 V at 62.5 Hz. The major source of the uncertainty at low frequencies in the conventional method is the voltage coefficient of the reference TVC, which is estimated by theoretical calculations for specially designed low-frequency TVCs [28]. As shown in table 1, the improvements in the uncertainty obtained by the differential sampling method along with the sampling DVM referred to the external timer were even more significant compared with those obtained by the conventional method based on the TVC.

Table 2 presents the comparison of the expanded uncertainties obtained by the three methods at the selected frequencies. Figure 5 plots the expanded uncertainties of the AC–DC difference measurements listed in table 2. Compared with the differential sampling method along with the sampling DVM referred to its internal clock, a few improvements in uncertainties were obtained at 1 Hz. However, the reductions in uncertainties were not as crucial as those at higher frequencies (10 Hz and 62.5 Hz) owing to the increased type-A uncertainty caused by the thermal ripple of the output voltage from the TVC. The improvements in uncertainty were the highest at the lowest frequency of 10 Hz compared with the conventional method, where the accuracy of the TVC reduced. In addition, it is worth noting that the values measured using the conventional method based on the TVC agreed with those obtained using the differential sampling to well within the evaluated uncertainty. This confirms that the theoretical estimation of the low-frequency AC–DC differences provides accurate calibrations and that the routine uncertainties at low frequencies might be too conservative.

4. Conclusions

We have extended the voltage range of the differential sampling system to an rms value of 10 V using the larger-scale PJVS chip. The modified sampling DVM with a 10 MHz reference clock enables us to significantly reduce the expanded uncertainty of the AC–DC difference measurements at low frequencies by preventing the incoherent sampling of differential voltages. The expanded uncertainty ($k = 2$) of the AC–DC difference measurements is reduced from 7.0 μV/V to 1.8 μV/V at a frequency of 62.5 Hz and from 8.0 μV/V to 4.4 μV/V at a frequency of 1 Hz. Given that higher voltages are available in a frequency range down to 1 Hz, the differential sampling system can be used for a wider range of metrological applications, and it is promising for low-frequency voltage measurements where the accuracy of the TVC is reduced.

Acknowledgments

We express our gratitude to S-F Chen of the Center for Measurement Standards, the Industrial Technology Research Institute, for his meticulous comments and stimulating discussions that we found immensely helpful. In addition, we are grateful to A. Ichinose for proofreading the manuscript.

ORCID iD

Yasutaka Amagai https://orcid.org/0000-0001-6816-8158

References

[1] Inglis B D 1992 Standards for AC–DC transfer *Metrologia* **29** 191
[2] Oldham N M, Avramov-Zamurovic S and Parker M E 1997 Exploring the low-frequency performance of thermal converters using circuit models and a digitally synthesized source *IEEE Trans. Instrum. Meas.* **46** 352
[3] Laiz H and Klonz M 1999 A simulation tool for the AC–DC transfer difference of thermal converters at low frequencies *IEEE Trans. Instrum. Meas.* **48** 1155
[4] Amagai Y and Fujiki H 2014 Improved electrothermal simulation for low-frequency characterization of a single-junction thermal converter *IEEE Trans. Instrum. Meas.* **63** 3011

[5] Swerlein R L 1991 A 10 ppm accurate digital AC measurement algorithm *Proc. NCSL (Albuquerque)* pp 17–36
[6] Kampik M, Laiz H and Klonz M 2000 Comparison of three accurate methods to measure AC voltage at low frequencies *IEEE Trans. Instrum. Meas.* **49** 429
[7] Ihlenfeld W G K, Mohns E, Bachmair H, Ramm G and Moser H 2003 Evaluation of the synchronous generation and sampling technique *IEEE Trans. Instrum. Meas.* **52** 371
[8] Henderson D, Williams J M and Yamada T 2012 Application of a Josephson quantum voltage source to the measurement of microsecond timescale settling time on the Agilent 3458A 8 1/2 digit voltmeter *Meas. Sci. Technol.* **23** 124006
[9] Hamilton C A 2000 Josephson voltage standards *Rev. Sci. Instrum.* **71** 3611
[10] Hamilton C A, Burroughs C J and Kautz R L 1995 Josephson D/A converter with fundamental accuracy *IEEE Trans. Instrum. Meas.* **44** 223
[11] Benz S P, Hamilton C A, Burroughs C J, Harvey T E and Christian L A 1997 Stable 1-volt programmable voltage standard *Appl. Phys. Lett.* **71** 1866
[12] Burroughs C J, Rüfenacht A, Benz S P, Dresselhaus P D, Waltrip B C and Nelson T L 2008 Error and transient analysis of stepwise-approximated sine waves generated by programmable Josephson voltage standards *IEEE Trans. Instrum. Meas.* **57** 1322
[13] Lee J, Behr R, Katkov A S and Palafox L L 2009 Modeling and measuring error contributions in stepwise synthesized Josephson sine waves *IEEE Trans. Instrum. Meas.* **58** 803
[14] Jeanneret B, Overney F, Callegaro L, Mortara A and Rüfenacht A 2009 Josephson-voltage-standard-locked sine wave synthesizer: margin evaluation and stability *IEEE Trans. Instrum. Meas.* **58** 791
[15] Williams J M, Henderson D, Patel P, Behr R and Palafox L 2007 Achieving sub-100-ns switching of programmable Josephson arrays *IEEE Trans. Instrum. Meas.* **56** 651
[16] Jeanneret B, Overney F, Rüfenacht A and Nissilä J 2010 Strong attenuation of the transients' effect in square waves synthesized with a programmable Josephson voltage standard *IEEE Trans. Instrum. Meas.* **59** 1894
[17] Behr R, Palafox L, Ramm G, Moser H and Melcher J 2007 Direct comparison of Josephson waveforms using an AC quantum voltmeter *IEEE Trans. Instrum. Meas.* **56** 235
[18] Rüfenacht A, Burroughs C J and Benz S P 2008 Precision sampling measurements using ac programmable Josephson voltage standards *Rev. Sci. Instrum.* **79** 044704
[19] Rüfenacht A, Overney F, Mortara A and Jeanneret B 2011 Thermal-transfer standard validation of the Josephson-voltage-standard-locked sine wave synthesizer *IEEE Trans. Instrum. Meas.* **60** 2372
[20] Palafox L, Behr R and Funck T 2010 AC–DC difference measurements relative to Josephson generated voltages *Proc. CPEM Dig.* (Daejeon) pp 91–2
[21] Lee J, Behr R, Palafox L, Katkov A, Schubert M, Starkloff M and Böck A C 2013 An AC quantum voltmeter based on a 10 V programmable Josephson array *Metrologia* **50** 612
[22] Budovsky I, Behr R, Palafox L, Djordjevic S and Hagen T 2012 Technique for the calibration of thermal voltage converters using a Josephson waveform synthesizer and a transconductance amplifier *Meas. Sci. Technol.* **23** 124005
[23] Séron O, Budovsky I, Djordjevic S, Hagen T, Behr R and Palafox L 2012 Precision ac–dc transfer measurements with a Josephson waveform synthesizer and a buffer amplifier *IEEE Trans. Instrum. Meas.* **61** 198
[24] Amagai Y, Maruyama M and Fujiki H 2013 Low-frequency characterization in thermal converters using AC-programmable Josephson voltage standard system *IEEE Trans. Instrum. Meas.* **62** 1621
[25] Yamamori H, Yamada T, Sasaki H and Shoji A 2008 A 10 V programmable Josephson voltage standard circuit with a maximum output of 20 V *Supercond. Sci. Technol.* **21** 105007
[26] Takahashi H, Maruyama M, Amagai Y, Yamamori H, Kaneko N-H and Kiryu S 2015 Heat transfer analysis of a programmable Josephson voltage standard chip operated with a mechanical cooler *Physica C: Supercond. Appl.* **518** 89
[27] Chen S-F, Amagai Y, Maruyama M and Kaneko N-H 2015 Uncertainty evaluation of a 10 V rms sampling measurement system using AC-programmable Josephson voltage standard *IEEE Trans. Instrum. Meas.* **64** 3308
[28] Sasaki H, Takahashi K, Klonz M and Endo T 1993 High-precision AC–DC transfer standards at ETL *IEEE Trans. Instrum. Meas.* **42** 603